

# Modelling a Saturating Function of Signals Released in Irradiation Bystander Effects

Fuaada Mohd Siam, Muhamad Hanis Nasir, Hamizah Rashid

<sup>1</sup>Department of Mathematical Sciences, Faculty of Science, Universiti Teknologi Malaysia, 81310 Johor Bahru, Johor, Malaysia

## ABSTRACT

*Mechanisms of mammalian cell killing effects produced by irradiation are complex processes and it is vitally importance to understand the phenomenon. In this research, models of survival fraction of targeted and bystander cells are employed, with modification on the signaling factors. The models are a type of two-dimensional vector that structure a population cell depends on the double-strand breaks (DSBs) and mis-repair DSBs count ( $k$  and  $m$ , respectively). Data fitting and parameter estimation are used as model calibration. Then, by using the estimated parameters, the model simulation shows a good fit against the experimental data with a sum of absolute error (SAE) of 0.0355 and 0.1542, respectively. These errors confirmed that the models are successfully depicted the actual measurement of targeted and bystander effects.*

**Keywords:** Irradiation, targeted cells, bystander cells, two-structured ODEs, *fminsearchbnd*.

## I. INTRODUCTION

Human are commonly exposed to irradiation, whether consciously or accidentally [1]. As the incidence happened in Kim Kim River, Malaysia, an irresponsible authority dumped the toxic waste (radioactive) into the river illegally and affecting nearby people majorly primary students [2]. Many of them were warded due to the symptom of eyes or lung sick and breathing difficulty. These toxic waste is in category of  $\alpha$ -emitting materials that taken by body through breathing, drinking or eating, therefore the internal tissues are exposed directly and may cause biological damage [3].

When irradiation material interacts with biological matters, energy is deposited and chemical bond such as deoxyribonucleic acid (DNA) are damaged [4]–[5]. It is known that exposure to irradiation will increase the risk of DNA mutations and cancer development [6]–[7]. For instance, overexposure to the sun's ultraviolet rays can cause skin cancer. On the other hand, a laser, a device that can emit ultraviolet rays is useful in medicine; for example, it is used for cataract treatment [8].

In clinical perspective, irradiation is used in radiotherapy treatment for tumour control with side effects on bystander cells, which include inflammation in irradiated and nearby regions [9]. The intensity of irradiation is measured by the amount of energy deposited per unit mass. The standard unit of absorbed dose is Gray (Gy) such that 1 Gy = 1 joule per kilogram [10]. The aim of radiotherapy is to target the unwanted cells and avoid damage the bystander cells as much as possible. However, the bystander cells got affected due to intercellular communication between the irradiated cells and bystander cells [11]–[12]. The gap junctions of intercellular communication facilitate the transfer of small molecules for up to 1kDa between the cytoplasm of adjacent cells [13]. Thus, cells which are not in the targeted field of irradiation show high levels of mutations, chromosomal aberrations, and membrane signaling changes [14].

Irradiation exposure produce various types of damage. Typically, the major problem in the DNA double helix is DNA breaks: single-strand breaks and double-strand breaks (DSBs) in the arms of chromosomes [15]. Single-strand breaks are not really harmful to the cells and not involved in cell killing, but it can cause a mutation. Whereas, DSBs are considered as the most biologically damaging lesions produced. If several DSBs are produced, incorrect rejoining of the ends can take place leading to chromosome aberrations, carcinogenesis, mutation, and cell death [16].

Cell death can be measured in various ways. One measure of cell death is non-clonogenic cell or reproductive cell death; which means the loss of ability to divide and make colonies. This definition is particularly relevant in the context of radiobiology and cancer therapy since any tumour cell which has an ability to produce progeny results in the failure of tumour control. In the recent literature, the major mechanisms of mammalian cell death are thought to be apoptosis and necrosis [17]. Apoptosis (also known as programmed cell death) represents death by suicide. It is important process to remove unwanted or damaged cells in order to maintain a tissue homeostasis. Alteration in the apoptosis control is responsible for many human

diseases, including cancers. In contrast to apoptosis, necrosis is unprogrammed cell death due to unexpected cell damage. During necrosis, the cell swells and disruption of plasma membrane will cause a tissue injury. Some cells that pass through mitosis with large chromosome aberration may then die by apoptosis, necrosis, or senescence [18]. Senescence here by means a natural process of aging by which the cells loss the ability to divide.

DSB formation induces two separate but interrelated responses; the DSB repair processes pathway and signal transduction processes that can lead to cell cycle arrest and apoptosis. There is a group of proteins that recognize damage-induced DNA DSBs. There is evidence that  $\gamma$ -H2AX foci which can be visualized by using fluorescence microscopy technique, is a biomarker for DNA DSBs [19]–[20]. After DSBs formation, histone H2AX is phosphorylated by phosphoinositide-3-kinase-related protein kinase family at the sites of DSBs, which are important in cellular response to DNA damage. There are two major types of DSB repair pathways: non-homologous end joining which represents end-to-end joining, and homologous recombination repair which also known as template-assisted repair [20].

Apart from irradiation exposure that include cell killing and mutations that may lead to the induction of malignant transformation in targeted cells, irradiation also enhance the secondary effects in bystander cells [21]. Bystander effects is a complex of effects that include mutations, chromosomal aberrations, micronuclei formation, and cell death. There is ample evidence that bystander effects involve cell communication through gap junctions of intercellular communication or via soluble factors released by the irradiated cells [19].

A number of candidates of the soluble signaling molecules have been identified. These include reactive oxygen species, nitric oxide, interleukin-6, interleukin-8, and transforming growth factor- $\beta$ 1 [22]. After irradiation, levels of these molecules are found to be increased in the growth medium of irradiated cells. It is found that the medium conditioned on cells targeted, with undamaged tumour and senescent cells, contained high level of nitric oxide and transforming growth factor-beta [23]. These signals molecules result in an elevated level of DSBs in bystander cells.

The DNA damage on the targeted cells is the main target of irradiation but it is now accepted that the final outcome of irradiation is not restricted to the targeted area of irradiation only [21]–[22]–[23]–[24]–[25], see Figure 1. The actual mechanism underlying the targeted and bystander effects is still open for debated, however, it is not our intention to discuss the overall mechanism

of irradiation effects on mammalian cells.

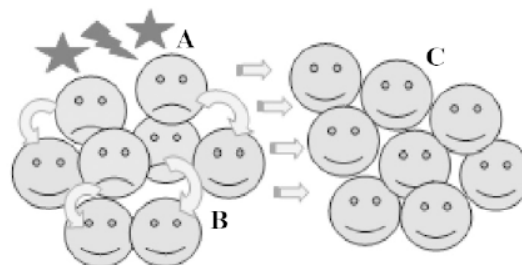


**Figure 1.** Region A is the targeted cells, while Region B and C are the bystander cells [25]. The arrows represent bystander signals.

In this research, we concentrated on two modelling of irradiation effects, which includes targeted effects model and bystander effects model. We calibrated the models with the experimental data by Yang et al. [26] and observed how well the model fits with the actual data. Next section provides the data of targeted and bystander cells and two appropriate models are discussed. Then, the parameter estimation is implemented into the models and the corresponding results are presented.

## II. METHODOLOGY

### A. Data

We employed two types of data that are survival fraction of targeted cells and bystander cells, as shown in Figure 2.

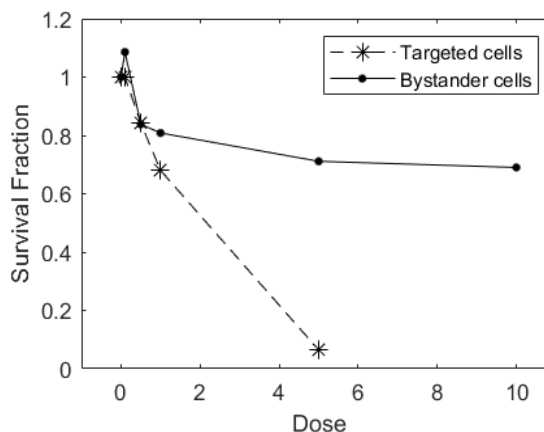


**Figure 2.** Experimental data of targeted and bystander cells (adapted from [16]).

Yang et al. [26] conducted an experiment on both survival fraction of targeted cells and bystander cells using the transwell insert coculture system. The AGO1522 normal human fibroblast cells was used to investigate the process of medium-mediated bystander effects. In their methodology, the cells were cultured in both plates and permeable membrane inserts where both

targeted cells and bystander normal human fibroblast cells shared the same medium, see Figure 3. Their findings show that there are some signaling pathways between the targeted cells and bystander cells that resulted in induction of DNA damage in bystander cells [26].

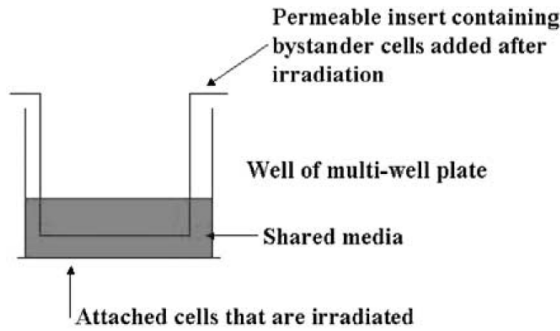


Figure 3. The transwell insert coculture system [26].

Many experimental observations revealed that the  $\gamma$ -H2AX foci are detected in bystander cells, which leads to agreement that there are DSBs in bystander cells after irradiation effects [19].

In targeted irradiation cells, the survival fraction decreases as higher dose is given to the targeted cells. However, the survival fraction in bystander cells that affected by bystander signals only follow dose dependency at low dose. At high dose, survival fraction of bystander cells remain steady and not gradually decreases as the survival fraction of targeted cells. These experimental data are used as model calibration on the model of targeted irradiation effects, as well as bystander irradiation effects.

**B. The Targeted Model of Irradiation Damage**

We first recall Siam et al. [27] model that represents the damage effects on cells after hit by irradiation as the DSBs count in each cell. The mean of DSBs count is described by Poisson distribution with mean,  $\mu_1 = \delta D$  where  $\delta$  is the cell’s radiosensitivity (DSBs · Gy-1) and D is irradiation dose. Immediately after irradiation, the DSBs damage produced in each cell and the targeted cells are grouped mathematically as  $T_{k,m}$ , with k as the DSBs count and m is the number of mis-repair DSBs. The group of targeted cells,  $T_{k,m}$  is represented as follows:

$$T'_{k,m}(t) = -d_1(k,m)T_{k,m}(t) - r_1(k)T_{k,m}(t) + \rho_1 r_1(k+1)T_{k+1,m}(t) + (1 - \rho_1) r_1(k+1)T_{k+1,m-1} \tag{1}$$

where  $d_1$  is the death rate of targeted cells ( $t-1$ ),  $r_1$  is the repair rate of targeted cells ( $t-1$ ) and  $\rho_1$  is the probability of successfully repair 1 DSB for targeted cells. The death rate is  $d_1(k,m) = (\alpha_1 m + \beta_1 k^2)$ , where  $\alpha_1$  is the death rate with respect to number of mis-repair DSBs and  $\beta_1$  is the death rate due to lethal DSBs aberration. The repair rate is described by Michelis-Menten function,  $r_1(k) = [(\sigma_1 k)/(\eta_1 + k)]$  where  $\sigma_1$  is the repair rate and  $\eta_1$  is the steepness curve of repair rate.

This type of model has a general solution in the form of  $T(t) = \exp \{A(t - t_0)\} T_0$ , where T is the vector contain group of targeted cell  $T_{k,m}$  for  $k + m \leq k_{max}$ , A is the coefficient matrix and  $T_0$  is the initial condition at  $t_0$ . Hence, the survival fraction of targeted cells is computed as follows:

$$SFT = \frac{\sum_{m=0}^{k_{max}-k} \sum_{k=0}^{k_{max}} T_{k,m}(t)}{\sum_{m=0}^{k_{max}-k} \sum_{k=0}^{k_{max}} T_{k,m}(0)} \tag{2}$$

In the effect of targeted cells towards irradiation, it is common to relate with Linear-Quadratic (LQ) formalism [28, 29]. LQ formalism exhibits as follows:

$$SFT = \exp\{-\alpha D - \beta D^2\} \tag{3}$$

where SFT is survival fraction of targeted irradiation and factors  $\alpha$  and  $\beta$  are in units of Gy-1 and Gy-2, respectively. In a cell culture, high proliferating cells are less sensitive to irradiation and have high  $\alpha/\beta$  ratio (6-14 Gy), while slow proliferating cells are very sensitive and have low  $\alpha/\beta$  ratio (1.5-5 Gy).

**C. The bystander model of irradiation damage**

Siam and Nasir [22] developed the model of survival fraction for bystander cells. The DSBs produced in each bystander cell is due to bystander signals released by the targeted cells. In this work, we improve the bystander signals model by introducing a saturating function of amount of bystander signals released as  $[(cD)/(\eta_2 + D)]$  with respect to irradiation dose (D). Then, the DSBs produced on bystander cells upon reacted with bystander signals is described by Poisson distribution with mean:

$$\mu_2 = \vartheta \left( \frac{cD}{\eta_2 + D} \right) \tag{4}$$

where  $\vartheta$  is the factor of DSBs induction on bystander

cells (DSBs · μM<sup>-1</sup>), *c* is the signals amount (μM) and η<sub>2</sub> is the steepness curve of bystander signals.

After the DSBs formed in each bystander cell, they will be grouped mathematically according to DSBs count and number of mis-repair DSBs, *B<sub>k,m</sub>*. The group of bystander cells, *B<sub>k,m</sub>* is represented as follows:

$$B'_{k,m}(t) = -d_2(k,m)B_{k,m}(t) - r_2(k,\omega)B_{k,m}(t) + \rho_2 r_2(k+1,\omega)B_{k+1,m}(t) + (1-\rho_2)r_2(k+1,\omega)B_{k+1,m-1}, \quad (5)$$

where *d<sub>2</sub>* is the death rate of bystander cells (*t*<sup>-1</sup>), *r<sub>2</sub>* is the repair rate of bystander cells (*t*<sup>-1</sup>) and ρ<sub>2</sub> is the probability of successfully repair 1 DSB for bystander cells. The death mechanism of bystander cells is assumed same as the targeted cells, *d<sub>2</sub>(k,m) = (α<sub>2</sub>m + β<sub>2</sub>k<sup>2</sup>)* with parameter α<sub>2</sub> and β<sub>2</sub> is rate of cell deaths due to mis-repair and lethal DSBs aberration in bystander cells, respectively. The repair mechanism is described as directly proportional to number of DSBs with the delay, *r<sub>2</sub>(k,ω) = σ<sub>2</sub>kω*, where σ<sub>2</sub> is the repair rate and ω is the heavy-side step function:

$$\omega(t) = \begin{cases} 0 & \text{if } t \leq \tau, \\ 1 & \text{if } t > \tau, \end{cases} \quad (6)$$

where τ is the delay activation of repair mechanism [30].

This model has an exact solution in form of **B**(*t*) = exp {**A**(*t - t<sub>0</sub>*)}**B**<sub>0</sub>, where **B** is vector of group of bystander cells, *B<sub>k,m</sub>* for *k + m ≤ k<sub>max</sub>*. Hence, the survival fraction of bystander cells is computed as follows:

$$SFB = \frac{\sum_{m=0}^{k_{max}-k} \sum_{k=0}^{k_{max}} B_{k,m}(t)}{\sum_{m=0}^{k_{max}-k} \sum_{k=0}^{k_{max}} B_{k,m}(0)}. \quad (7)$$

Both models, Equation (2) and (7) will return the value of survival fraction that is in range of 0 to 1, which indicates the ratio of cells that remain alive.

### III. RESULT AND DISCUSSION

The analysis for both models involved parameter estimation and data fitting towards the survival fraction of targeted and bystander cells. The Nelder-Mead Simplex optimization which is a built-in MATLAB function called “*fminsearchbnd*” is used in data fitting. The sum of absolute error (SAE) in data fitting is defined as follows:

$$SAE = \sum_{i=1}^n |z_i - \bar{z}_i|, \quad (8)$$

where *z<sub>i</sub>* is the experimental data,  $\bar{z}_i$  is the mathematical model data for *i* = 1, 2, ..., *n* set of available data. The experimental data shown in Figure 2 is used into fitting with both models. According to the biological significance, the boundary of each parameter is set reasonably in Table 1.

**Table 1.** Estimation of parameter and SAE value

Targeted model		Bystander model	
Parameter Interval	Estimated parameter	Parameter Interval	Estimated parameter
δ [0.01, 10]	1.1947	ρ [0.001, 10]	1.4121
ρ <sub>1</sub> [0, 1]	0.8854	<i>c</i> [0.1, 1.5]	0.6452
α <sub>1</sub> [0.001, 1]	0.4324	η <sub>2</sub> [0.001, 5]	0.8634
β <sub>1</sub> [0.001, 1]	0.2134	ρ <sub>2</sub> [0, 1]	0.6453
σ <sub>1</sub> [0.01, 5]	3.9001	α <sub>2</sub> [0.001, 1]	0.8961
η <sub>1</sub> [1, 5]	2.7484	β <sub>2</sub> [0.001, 1]	0.3946
LQ	α [0, 1]	σ <sub>2</sub> [0.01, 5]	4.9110
	β [0, 1]	τ [0.05, 0.2]	0.0948
SAE	0.0355	SAE	0.1542

By using the estimated parameters, model simulations are provided in Figure 4 and it shows that the models provide good fits towards experimental data.

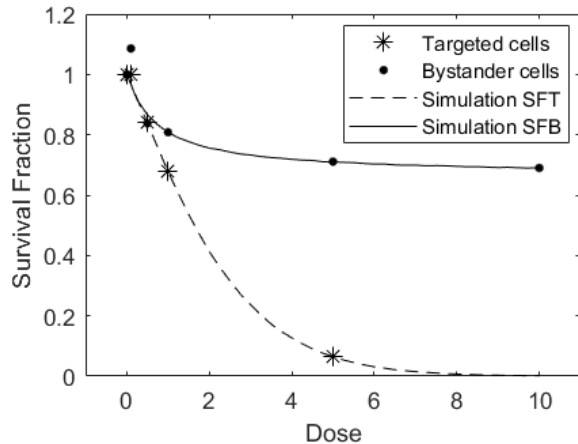


**Figure 4.** Model simulation using the estimated parameters

against the experimental data.

For the bystander signals, we observed that at high dose the signals released is saturated to  $0.6452 \mu M$ . The bystander signals contributed to the average DSBs induced with mean,  $\mu_2 = 1.4121[(0.6452 D)/(0.8634+D)]$  in bystander cells. Whereas, in targeted cells, the average DSBs induced,  $\mu_1 = 1.1947D$  is not a high amount contributed to the DSBs load after irradiation. It can be relating to the estimated parameters in LQ formalism (3), the ratio of  $\alpha/\beta$  is 7.9730 Gray shows that the targeted cells have high proliferating and are less sensitive to irradiation. In the LQ formalism,  $\alpha/\beta$  ratio is a dose in Gray which is used to describe the effect of irradiation dose and fractionation. In fractionated condition, a total dose of radiotherapy is broken into smaller amounts and administered over a period of time, rather than a single larger dose [31]. The  $\alpha/\beta$  ratio describing the tissue's response to dose fractionation. There is evidence that tissues with low  $\alpha/\beta$  ratio are usually characterized as late responding tissues and show high sensitivity to fractionation changes, in contrast for tissue with high  $\alpha/\beta$  ratio is characterized as early responding tissues [32]. Modelling implication of this matter could be explored further.

Mathematical and statistical modelling have played a crucial role to give a vital information to determine the optimal radiotherapy schedule for a patient. The LQ formalism is widely used for analyzing cell survival in vitro and in vivo in both experimental and clinical radiobiology. Clinical radiobiology such as tumour control probability (TCP) is the probability that no malignant cells are left in a specified location after irradiation [33]–[34]. The LQ formalism provides a formula for the cell survival fraction that can be used for the prediction of TCP. The standard model of local tumour control is given as:

$$TCP = \exp\{-N_0 \exp\{-\alpha D - \beta D^2\}\}, \quad (9)$$

where  $N_0$  is the total number of clonogens per tumour before irradiation and the second exponent come from LQ formalism [35]. TCP determines the optimal treatment strategy at which the dose to the tumour is increased and more malignant cells will die without increasing the cell killing effect to bystander cells.

This exercise concluded in here is an outline to two plausible models that can be fitted to experimental data. We have relied on very limited possible intervals for the parameters values. This is certainly an important issue in modelling as we want to know the information from the models analyzed. Limitation that the model does not

allow repopulation, quiescent state and any representation of the cell cycle put the models as not so much a final model due to many things are unknown, but a modelling framework that can be developed in future.

#### IV. CONCLUSION

A model of targeted effects is adopted, while a bystander model is improved in term of signals released. A completion of the modelling is involved data fitting from experimental measurement. The parameter estimation using SAE minimization gives a good simulation against the experimental data. The estimated parameters can be valuable for radiobiologist in order to design new experimental procedure and reduce animal use. Overall, the results show that the model provides a mechanistic explanation for the irradiation effects phenomenon for both targeted and bystander effects in the aspect of cellular activity, which can be manipulated experimentally.

#### ACKNOWLEDGEMENT

This work was financially supported by Universiti Teknologi Malaysia under FRGS: R.J130000.7826.4F889 and Ministry of Education Malaysia. We are grateful to the editor and anonymous referees for comments which substantially improved the article.

#### REFERENCES

- [1] Squillaro, T., Galano, G., De Rosa, R., Peluso, G. & Galderisi, U. 2018. "Concise review: The effect of low-dose ionizing radiation on stem cell biology: A contribution to radiation risk. *Stem Cells*". 36(8), 1146-1153.
- [2] Hussein, I. N. A. 2019. "Pusat bencana Sungai Kim Kim tutup". (accessed on May 27, 2019). Retrieved from <https://www.hmetro.com.my/utama/2019/03/435782/pusat-bencana-sungai-kim-kim-tutup>.
- [3] Nies, H., 2018. "Pollution with radioactive substances. In *Handbook on Marine Environment Protection*" (pp. 413-427). Springer, Cham.
- [4] Schofield, P. N. & Kondratowicz, M. 2018. "Evolving paradigms for the biological response to low dose ionizing radiation; the role of epigenetics?". *International Journal of Radiation Biology*. 94(8), 769-781.
- [5] Burgio, E., Piscitelli, P. & Migliore, L. 2018. "Ionizing radiation and human health: Reviewing models of exposure and mechanisms of cellular damage". An epigenetic perspective. *International Journal of Environmental Research and Public Health*. 15(9), 1971.
- [6] Nikjoo, H., Emfietzoglou, D., Liamsuwan, T., Taleei, R., Liljequist, D. & Uehara, S. 2016. "Radiation track, DNA damage and response—a review." *Reports on Progress in Physics*. 79(11), 116601.
- [7] Hall, J., Jeggo, P. A., West, C., Gomolka, M., Quintens, R., Badie, C., Laurent, O., Aerts, A., Anastasov, N., Azimzadeh, O. & Azizova, T. 2017. "Ionizing radiation biomarkers in epidemiological studies—an update". *Mutation Research/Reviews in Mutation Research*, 771, 59-84.

- [8] Topete, A., Serro, A. P. and Saramago, B., 2019. “Dual drug delivery from intraocular lens material for prophylaxis of endophthalmitis in cataract surgery”. *International journal of pharmaceuticals*, 558, pp.43-52.
- [9] Li, M., You, L., Xue, J. & Lu, Y. 2018. “Ionizing radiation-induced cellular senescence in normal, [11] Arora, S., Heyza, J., Chalfin, E., Ruch, R. & Patrick, S. 2018. “Gap junction intercellular communication positively regulates cisplatin toxicity by inducing DNA damage through bystander signaling. *Cancers*”. 10(10), 368.
- [12] Kobayashi, A., Autsavapromporn, N., Ahmad, T. A. F., Oikawa, M., Homma-Takeda, S., Furusawa, Y., Wang, J. & Konishi, T., 2018. “Bystander WI-38 cells modulate DNA double-strand break repair in microbeam-targeted A549 cells through gap junction intercellular communication”. *Radiation Protection Dosimetry*.
- [13] Beckmann, A., Hainz, N., Tschernig, T. and Meier, C., 2019. “Facets of communication: Gap junction ultrastructure and function in cancer stem cells and tumor cells”. *Cancers*, 11(3), p.288.
- [14] Nasir, M. H., & Siam, F. M. 2017. Mini-review: “Recent updates on the mathematical modelling of radiation-induced bystander effects”. *Malaysian Journal of Fundamental and Applied Sciences*. 13(2), 103-108.
- [15] Gonon, G., Villagrasa, C., Voisin, P., Meylan, S., Bueno, M., Benadjaoud, M. A., Tang, N., Langner, F., Rabus, H., Barquinero, J. F. and Giesen, U., 2019. “From energy deposition of ionizing radiation to cell damage signaling: Benchmarking simulations by measured yields of initial DNA damage after ion microbeam irradiation”. *Radiation research*, 191(6), pp.566-584.
- [16] McMahan, S. J. and Prise, K. M., 2019. “Mechanistic modelling of radiation responses”. *Cancers*, 11(2), p.205.
- [17] Zhao, H., Zhuang, Y., Li, R., Liu, Y., Mei, Z., He, Z., Zhou, F. and Zhou, Y., 2019. “Effects of different doses of X ray irradiation on cell apoptosis, cell cycle, DNA damage repair and glycolysis in HeLa cells”. *Oncology letters*, 17(1), pp.42-54.
- [18] Jiang, X., Xu, J. and Gore, J. C., 2019. “Quantitative temporal diffusion spectroscopy as an early imaging biomarker of radiation therapeutic response in gliomas: A preclinical proof of concept”. *Advances in radiation oncology*, 4(2), pp.367-376.
- [19] Wang, H., Yu, K. N., Hou, J., Liu, Q. & Han, W. 2015. “Radiation-induced bystander effect: Early process and rapid assessment”. *Cancer Letters*. 356, 137-144.
- [20] Perez, R. L., Nicolay, N. H., Wolf, J. C., Frister, M., Schmezer, P., Weber, K. J. and Huber, P. E., 2019. “DNA damage response of clinical carbon ion versus photon radiation in human glioblastoma cells”. *Radiotherapy and Oncology*, 133, pp.77-86.
- [21] Subhashree, M., Venkateswarlu, R., Karthik, K., Shangamithra, V., & Venkatachalam, P. 2017. “DNA damage and the bystander response in tumor and normal cells exposed to X-rays”. *Mutation Research/Genetic Toxicology and Environmental Mutagenesis*. 821, 20-27.
- [22] Siam, F. M. & Nasir, M. H. 2018. “Mechanistic model of radiation-induced bystander effects to cells using structured population approach”. *MATEMATIKA*. 34(3), 149-165.
- [23] Han, W., Chen, S., Yu, K. N. & Wu, L. 2010. “Nitric oxide mediated DNA double strand breaks induced in proliferating bystander cells after  $\alpha$ -particle irradiation”. *Mutation non-transformed cells and the involved DNA damage response: A mini review*”. *Frontiers in pharmacology*. 9, 522.
- [10] Rich, S. E. and Dharmarajan, K. V., 2019. “Introduction to radiation therapy. In *Essentials of Interventional Cancer Pain Management*” (pp. 319-328). Springer, Cham.
- Research/Fundamental and Molecular Mechanisms of Mutagenesis. 684(1-2), 81-89.
- [24] Nasir, J. 2017. “Use of E18 cell model to quantify DNA strand break associated bystander effect (DSB-ABE)”. *Journal of Carcinogenesis and Mutagenesis*. 8(295), 27-29.
- [25] Verma, N. and Tiku, A. B., 2017. “Significance and nature of bystander responses induced by various agents”. *Mutation Research/Reviews in Mutation Research*, 773, 104-121.
- [26] Yang, H., Asaad, N. & Held, K. D. 2005. “Medium-mediated intercellular communication is involved in bystander responses of X-ray-irradiated normal human fibroblasts”. *Oncogene*. 24(12), 2096.
- [27] Siam, F. M., Grinfeld, M., Bahar, A., Rahman, H. A., Ahmad, H. & Johar, F. (2018). “A mechanistic model of high dose irradiation damage”. *Mathematics and Computers in Simulation*. 151, 156-168.
- [28] Jalalimanesh, A., Haghighi, H. S., Ahmadi, A. & Soltani, M. 2017. “Simulation-based optimization of radiotherapy: Agent-based modeling and reinforcement learning”. *Mathematics and Computers in Simulation*. 133, 235-248.
- [29] Farayola, M. F., Shafie, S. and Siam, F. M., 2019. “Population dynamics of normal and cancer cells under radiotherapy”. *Science Proceedings Series*, 1(2), pp.51-54.
- [30] Nasir, M. H. & Siam, F. M. 2019. “Simulation and sensitivity analysis on the parameter of non-targeted irradiation effects model”. *Jurnal Teknologi*. 81(1): 133-142.
- [31] Arnold, K. M., Flynn, N. J., Raben, A., Romak, L., Yu, Y., Dicker, A. P., Mourtada, F. and Sims-Mourtada, J., 2018. “The impact of radiation on the tumor microenvironment: Effect of dose and fractionation schedules”. *Cancer growth and metastasis*, 11, p.1179064418761639.
- [32] Lewin, T. D., Maini, P. K., Moros, E. G., Enderling, H. and Byrne, H. M., 2018. “The evolution of tumour composition during fractionated radiotherapy: Implications for outcome”. *Bulletin of Mathematical Biology*, 80(5), 1207-1235.
- [33] Casares-Magaz, O., Raidou, R. G., Rørvik, J., Vilanova, A. and Muren, L.P., 2018. “Uncertainty evaluation of image-based tumour control probability models in radiotherapy of prostate cancer using a visual analytic tool”. *Physics and Imaging in Radiation Oncology*, 5, pp.5-8.
- [34] Her, E. J., Reynolds, H. M., Mears, C., Williams, S., Moorehouse, C., Millar, J. L., Ebert, M. A. and Haworth, A., 2018. “Radiobiological parameters in a tumour control probability model for prostate cancer LDR brachytherapy”. *Physics in Medicine & Biology*, 63(13), p.135011.
- [35] Hillen, T., De VrleS, G., Gong, J. and Finlay, C., 2010. “From cell population models to tumor control probability: Including cell cycle effects”. *Acta Oncologica*, 49(8), pp.1315-1323.